

DIAGRAMMATIC EXPANSIONS FOR THE YANG-MILLS GROUND STATE

Hue Sun CHAN

*Lawrence Berkeley Laboratory and Department of Physics, University of California,
Berkeley, California 94720, USA*

Received 13 March 1986

Starting from the finite-time action formulation of the temporal gauge, we derive diagrammatic rules for the perturbative evaluation of the Yang-Mills ground state wave functional and energy to all orders. The perturbative expansions are also easily reorganized into semi-classical expansions. As an application, the ground state wave functional through first non-trivial order is explicitly computed. We also speculate on the use of gauge invariance to improve perturbation theory.

1. Introduction

The continuum Yang-Mills ground state wave functional and energy has been periodically studied [1–4]. Recently, Hatfield [4] emphasized that usual hamiltonian perturbation theory is problematic in gauge theory because the gauge-invariant eigenstates are not normalizable in the unrestricted field space. To obtain the ground state through first non-trivial order, Hatfield therefore directly solved the functional Schrödinger equation with the Gauss' law constraint. However, his method involves certain ansätze already at first order and no attempt is made to find a systematic approach at higher orders.

In this paper, we develop two systematic diagrammatic expansions for the ground state wave functional and ground state energy to all orders. The method is based on finite-time functional integral representations of the ground state wave functional [5] and the finite-time temporal gauge perturbation theory [6–9]. The new perturbation series may also be organized into semi-classical expansions, in which the order of \hbar counts the number of loops in the diagrams.

As an application of the diagrammatic rules, we computed the ground state wave functional through first non-trivial order, and the result is in agreement with Hatfield. We also introduce the notion of “gauge-invariant completion”, in which gauge invariance is used to improve perturbation theory. As an example, a manifestly gauge-invariant form which agrees with the first-order result is obtained.

The organization of this paper is as follows. In sect. 2, we begin with two functional integral representations of the ground state wave functional and energy. In sect. 3, we give diagrammatic rules for their perturbative computation, and discuss the semi-classical expansions. In sect. 4, the ground state through first order in g is explicitly computed, and gauge-invariant completions of the result are discussed.

2. Functional representations of the ground state

Our first functional integral representation of the ground state is based on the smeared temporal gauge action formulation of Rossi and Testa [6, 7] and Chan [9]. The starting point is the euclidean functional integral

$$Z_\Phi[A; T] \equiv \int \mathcal{D}F \Phi^{(\epsilon)}[F] \int_{A'(x, -T)=A(x)}^{A'(x, 0)=F(x)} \mathcal{D}A' e^{-S_T[A']/\hbar}. \quad (2.1)$$

Here, S_T is the usual finite time QCD action,

$$S_T[A] = \frac{1}{2} \int_{-T}^0 dt \int d\mathbf{x} (\dot{A}_i^a \dot{A}_i^a + B_i^a B_i^a), \quad (2.2)$$

$$B_i^a(A) = \frac{1}{2} \epsilon_{ijk} F_{jk}^a(A), \quad F_{jk}^a(A) = \partial_j A_k^a - \partial_k A_j^a - gf^{abc} A_j^b A_k^c, \quad (2.3)$$

and we have used the particular gauge-invariant final-state smearing functional [9]

$$\Phi^{(\epsilon)}[F] = \exp \left[-\frac{1}{2\hbar\epsilon^2} \int d\mathbf{x} B_i^a(F) B_i^a(F) \right], \quad 0 < \epsilon^2 < \infty, \quad (2.4)$$

for which Feynman rules have recently been obtained [9]. As in ref. [7], the functional Z_Φ may be expanded in terms of gauge-invariant physical states ψ_n ,

$$Z_\Phi[A; T] = \sum_n c_n \psi_n[A] e^{-E_n T/\hbar}, \quad (2.5)$$

where c_n are constant coefficients independent of the gauge field. The states ψ_n satisfy the functional Schrödinger equation

$$\frac{1}{2} \int d\mathbf{x} \left[-\hbar^2 \frac{\delta}{\delta A_i^a(\mathbf{x})} \frac{\delta}{\delta A_i^a(\mathbf{x})} + B_i^a(\mathbf{x}) B_i^a(\mathbf{x}) \right] \psi_n[A] = E_n \psi_n[A] \quad (2.6)$$

and the Gauss' law condition

$$D_i^{ab} \frac{\delta}{\delta A_i^b} \psi_n[A] = 0, \quad (2.7)$$

where $D_i^{ab} \equiv \delta^{ab} \partial_i + gf^{abc} A_i^c$ is the covariant derivative.

From the expansion (2.5), it is easy to see that a functional representation of the ground state

$$\psi_0[A] \approx \exp\left[\frac{1}{\hbar} W[A]\right] \tag{2.8}$$

is given by

$$W[A] = \hbar \lim_{T \rightarrow \infty} \left[\ln \frac{Z_\phi[A; T]}{Z_\phi[0; T]} \right], \tag{2.9}$$

whereas a corresponding functional representation of the ground state energy is

$$E_0 = -\hbar \lim_{T \rightarrow \infty} \left[\frac{1}{T} \ln(Z_\phi[0; T]) \right]. \tag{2.10}$$

It should be emphasized here that the same information of the ground state can also be obtained from the partition function given by Rossi and Testa in appendix B of ref. [7]. However, as pointed out in ref. [9], the final-state smearing (2.4) provides simpler gauge-invariant expansions for perturbative analysis.

In the Rossi-Testa-Chan formulation above, the final-state smearing guarantees the gauge invariance of the states ψ_n in the expansion (2.5). Nevertheless, according to Feynman's argument [10] and a recent perturbative check [9], the gauge-invariant ground state should also be obtainable at large T even when the functional integrals are not smeared. More precisely, the functional integral representations

$$W[A] = \hbar \lim_{T \rightarrow \infty} \left[\ln \frac{Z[A, 0; T]}{Z[0, 0; T]} \right], \tag{2.11a}$$

$$E_0 = -\hbar \lim_{T \rightarrow \infty} \left[\frac{1}{T} \ln(Z[0, 0; T]) \right], \tag{2.11b}$$

with the unsmeared transition amplitude

$$Z[F, I; T] \equiv \int_{A(x, -T)=I}^{A(x, 0)=F} \mathcal{D}A e^{-S_T[A]/\hbar} \tag{2.12}$$

should provide results equivalent to those of eqs. (2.9)–(2.10). Subsequent computations will verify that this is in fact the case. The representations (2.11)–(2.12) are equivalent to representations used by Greensite and Halpern [5].

Our task is reduced to the perturbative evaluation of the two finite-time partition functions $Z_\phi[A; T]$ and $Z[A, 0; T]$. For this purpose, the Claudson-Halpern maps [11] provide a convenient method. By the Claudson-Halpern identity

$$Z[F, I; T] = e^{\pm(W[F] - W[I])} \left\langle e^{\pm \xi((A')^\pm)} \delta[(A')^\pm(\cdot, 0) - F(\cdot)] \right\rangle_\eta, \tag{2.13}$$

the quantities Z_ϕ and Z may be written as

$$Z_\phi[A; T] = e^{\mp W[A]} \left\langle \Phi[(A')^\pm(0)] e^{\pm W((A')^\pm(0))} \right\rangle_\eta, \tag{2.14a}$$

$$Z[A, 0; T] = e^{\pm W[A]} \left\langle \delta[(A')^\pm(\cdot, 0) - A(\cdot)] \right\rangle_\eta, \tag{2.14b}$$

where, following refs. [8, 9], we have ignored the function ξ , which is adequate for perturbative computations. In the above equations, the η -averages are performed with the gaussian Boltzmann factor

$$\exp\left[-\frac{1}{2}\int_{-T}^0 dt \int d\mathbf{x} \eta_i^a(\mathbf{x}, t) \eta_i^a(\mathbf{x}, t)\right], \quad (2.15)$$

while $(A')^\pm$ corresponds to either of the pair of Claudson-Halpern maps (with \hbar reinstated),

$$(\dot{A}')_i^{\pm a} = \mp B_i^a(A') + \sqrt{\hbar} \eta_i^a, \quad (2.16)$$

and W is the winding number.

The perturbative analysis of eqs. (2.14) is carried out by methods very similar to those of refs. [8, 9]: zeroth-order generating functionals are first computed by the zeroth-order Claudson-Halpern maps, the result being independent of which map was used. Higher order terms are then generated by differentiating these generating functionals with appropriate interaction terms. The zeroth-order computation results in the following expression for Z_Φ :

$$Z_\Phi[A; T] = \Gamma_\Phi^{(0)}[A; T] Z_\Phi^{(I)}\left[\frac{\delta}{\delta J}\right] Z_\Phi^{(0)J}[A; T]\Big|_{J=0}, \quad (2.17)$$

where*

$$\begin{aligned} \Gamma_\Phi^{(0)}[A; T] = & \exp\left[-V(N^2 - 1) \int (d\mathbf{p}) \ln \frac{p \sinh(Tp) + \epsilon^2 \cosh(Tp)}{\epsilon^2}\right] \\ & \times \exp\left[-\frac{1}{2\hbar} \int d\mathbf{x} A_i^{(T)a} \sqrt{-\nabla^2}\right. \\ & \left. \times \left\{ \frac{\sqrt{-\nabla^2} \cosh(T\sqrt{-\nabla^2}) + \epsilon^2 \sinh(T\sqrt{-\nabla^2})}{\sqrt{-\nabla^2} \sinh(T\sqrt{-\nabla^2}) + \epsilon^2 \cosh(T\sqrt{-\nabla^2})} \right\} A_i^{(T)a}\right], \quad (2.18) \end{aligned}$$

$$\begin{aligned} Z_\Phi^{(I)}\left[\frac{\delta}{\delta J}\right] = & \exp\left[\frac{1}{\hbar} \int_{-T}^0 dt \int d\mathbf{x} \left(1 + \frac{\delta(t)}{\epsilon^2}\right)\right. \\ & \left. \times \left\{ f^{abc} \frac{\delta}{\delta J_i^a} \frac{\delta}{\delta J_j^b} \partial_i \frac{\delta}{\delta J_j^c} - \frac{1}{4} g^2 f^{abefcde} \frac{\delta}{\delta J_i^a} \frac{\delta}{\delta J_j^b} \frac{\delta}{\delta J_j^c} \frac{\delta}{\delta J_j^d} \right\}\right], \quad (2.19) \end{aligned}$$

$$\begin{aligned} Z_\Phi^{(0)J}[A; T] = & \exp\left[\int_{-T}^0 dt \int d\mathbf{x} J_i^a(\mathbf{x}, t) P_i^a(\mathbf{x}, t)\right. \\ & \left. + \frac{1}{2} \int_{-T}^0 dt dt' \int d\mathbf{x} d\mathbf{x}' J_i^a(\mathbf{x}, t) \Delta_{ij}^\Phi(\mathbf{x}, t; \mathbf{x}', t') J_j^a(\mathbf{x}', t')\right]. \quad (2.20) \end{aligned}$$

* Throughout this paper, we adopt the convention $(d\mathbf{p}) \equiv d^3p/(2\pi)^3$ and $p \equiv \sqrt{\mathbf{p}^2}$.

In eqs. (2.17)–(2.18), $\Gamma_{\Phi}^{(0)}$ is obtained by a careful formal manipulation of the determinant that arises from the η -gaussian averaging. $V \equiv \int d\mathbf{x}$ is formally the spatial volume of the system, $V(N^2 - 1)f(d\mathbf{p})$ is formally the number of longitudinal degrees of freedom for $SU(N)$, and the superscript L[T] denotes longitudinal [transverse] projection of the field, as given by the usual projection operators \hat{L}_{ij} and \hat{T}_{ij} ,

$$A_i^{(L)a} = \hat{L}_{ij}A_j^a, \quad A_i^{(T)a} = \hat{T}_{ij}A_j^a. \quad (2.21)$$

In eq. (2.19), $Z_{\Phi}^{(I)}$ contains the interacting part of both the action and the final-state smearing functional $\Phi^{(\epsilon)}$, and is responsible for the vertex factors in the Feynman rules of fig. 1. In eq. (2.20), the field insertion $P_i^a(\mathbf{x}, t)$ is given by

$$P_i^a(\mathbf{x}, t) = \left[\hat{L}_{ij} + \frac{-\sqrt{-\nabla^2} \sinh(t\sqrt{-\nabla^2}) + \epsilon^2 \cosh(t\sqrt{-\nabla^2})}{\sqrt{-\nabla^2} \sinh(T\sqrt{-\nabla^2}) + \epsilon^2 \cosh(T\sqrt{-\nabla^2})} \hat{T}_{ij} \right] A_j^a(\mathbf{x}). \quad (2.22)$$

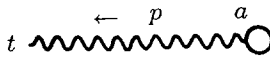
In the diagrammatic expansions to be discussed in the next section, this field insertion will be seen to provide the field dependence of the ground state wave functional. Diagrammatically, the momentum space field insertion $\tilde{P}_i^a(\mathbf{p}, t)$ (the spatial Fourier transform of $P_i^a(\mathbf{x}, t)$) is represented by a wavy line with a small circle attached, as shown in fig. 1a. Also in eq. (2.19), Δ_{ij}^{Φ} is the smeared finite-time propagator derived in ref. [9],

$$\begin{aligned} \Delta_{ij}^{\Phi}(\mathbf{x}, t; \mathbf{x}', t') = \hbar \left\{ \left[\theta(t' - t)(t + T) \hat{L}_{ij} + \frac{\theta(t' - t) \sinh[(t + T)\sqrt{-\nabla^2}]}{\sqrt{-\nabla^2} \sinh[T\sqrt{-\nabla^2}]} \right] \right. \\ \left. \times \left\{ -\sinh[t'\sqrt{-\nabla^2}] + \frac{\epsilon^2 \sinh[(t' + T)\sqrt{-\nabla^2}]}{\sqrt{-\nabla^2} \sinh[T\sqrt{-\nabla^2}] + \epsilon^2 \cosh[T\sqrt{-\nabla^2}]} \right\} \hat{T}_{ij} \right\} \\ \left. + (t \leftrightarrow t') \right\} \delta(\mathbf{x} - \mathbf{x}'). \quad (2.23) \end{aligned}$$

The corresponding momentum space propagator is represented by a wavy line in fig. 1b.

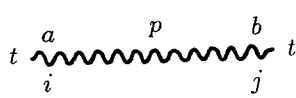
In the same manner, we also obtain the analogous expression for the unsmeared functional Z given in eq. (2.14b),

$$Z[A, 0; T] = \Gamma^{(0)}[A; T] Z^{(I)} \left[\frac{\delta}{\delta J} \right] Z^{(0)J}[A; T] \Big|_{J=0}, \quad (2.24)$$



$$= \tilde{P}_i^a(\vec{p}, t) \equiv [\hat{L}_{ij} + \frac{-p \sinh[tp] + \epsilon^2 \cosh[tp]}{p \sinh[Tp] + \epsilon^2 \cosh[Tp]} \hat{T}_{ij}] A_j^a(\vec{p})$$

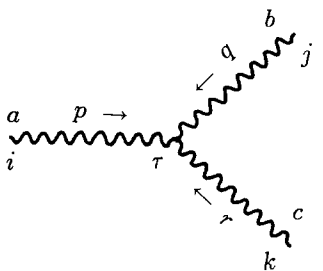
a



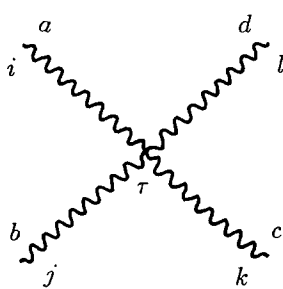
$$= \delta^{ab} \hbar \left\{ \theta(t' - t)(t + T) \hat{L}_{ij} + \theta(t' - t) \left\{ \frac{-\sinh[(t + T)p] \sinh[t'p]}{p \sinh[Tp]} + \frac{\epsilon^2 \sinh[(t + T)p] \sinh[(t' + T)p]}{p \sinh[Tp](p \sinh[Tp] + \epsilon^2 \cosh[Tp])} \right\} \hat{T}_{ij} \right\} + (t \leftrightarrow t') \right\}$$

$$= \tilde{S}_i^a(\vec{p}, t) \equiv \left[\frac{t + T}{T} \hat{L}_{ij} + \frac{\sinh[(t + T)p]}{\sinh[Tp]} \hat{T}_{ij} \right] A_j^a(\vec{p})$$

b



$$= -\frac{ig}{\hbar} f^{abc} \left[1 + \frac{\delta(\tau)}{\epsilon^2} \right] [(r - q)_i \delta_{jk} + (q - p)_k \delta_{ij} + (p - r)_j \delta_{ki}]$$



$$= -\frac{g^2}{\hbar} \left[1 + \frac{\delta(\tau)}{\epsilon^2} \right] [f^{abn} f^{cdn} (\delta_{ik} \delta_{jl} - \delta_{il} \delta_{jk}) + f^{cbn} f^{adn} (\delta_{ik} \delta_{jl} - \delta_{ij} \delta_{lk}) + f^{dbn} f^{can} (\delta_{lk} \delta_{ij} - \delta_{jk} \delta_{il})]$$

c

Fig. 1. Feynman rules for $\tilde{Z}_\phi[A; T]$ (smeared case). (a) Smeared field insertion. (b) Smeared propagator. (c) Smeared vertices.

where

$$\begin{aligned} \Gamma^{(0)}[A; T] &= \exp \left[-V(N^2 - 1) \int (d\mathbf{p}) \ln \{ 2 \sinh(T\mathbf{p}) \} \right] \\ &\quad \times \left(\frac{1}{T} \right)^{[V(N^2-1)f(d\mathbf{p})]/2} \exp \left[-\frac{1}{2\hbar T} \int d\mathbf{x} A_i^{(L)a} A_i^{(L)a} \right] \\ &\quad \times \exp \left[-\frac{1}{2\hbar} \int d\mathbf{x} A_i^{(T)a} \{ \sqrt{-\nabla^2} \coth [T\sqrt{-\nabla^2}] \} A_i^{(T)a} \right], \end{aligned} \quad (2.25)$$

$$\begin{aligned} Z^{(1)} \left[\frac{\delta}{\delta J} \right] &= \exp \left[\frac{1}{\hbar} \int_{-T}^0 dt \int d\mathbf{x} \left\{ f^{abc} \frac{\delta}{\delta J_i^a} \frac{\delta}{\delta J_j^b} \partial_i \frac{\delta}{\delta J_j^c} \right. \right. \\ &\quad \left. \left. - \frac{1}{4} g^2 f^{abefcde} \frac{\delta}{\delta J_i^a} \frac{\delta}{\delta J_j^b} \frac{\delta}{\delta J_i^c} \frac{\delta}{\delta J_j^d} \right\} \right], \end{aligned} \quad (2.26)$$

$$\begin{aligned} Z^{(0)J}[A; T] &= \exp \left[\int_{-T}^0 dt \int d\mathbf{x} J_i^a(\mathbf{x}, t) S_i^a(\mathbf{x}, t) \right. \\ &\quad \left. + \frac{1}{2} \int_{-T}^0 dt dt' \int d\mathbf{x} d\mathbf{x}' J_i^a(\mathbf{x}, t) \Delta_{ij}(\mathbf{x}, t; \mathbf{x}', t') J_j^a(\mathbf{x}', t') \right]. \end{aligned} \quad (2.27)$$

In the last equation,

$$S_i^a(\mathbf{x}, t) = \left[\frac{t+T}{T} \hat{L}_{ij} + \frac{\sinh[(t+T)\sqrt{-\nabla^2}]}{\sinh[T\sqrt{-\nabla^2}]} \hat{T}_{ij} \right] A_j^a(\mathbf{x}) \quad (2.28)$$

is the field insertion in the unsmeared formulation, while

$$\begin{aligned} \Delta_{ij}(\mathbf{x}, t; \mathbf{x}', t') &= \hbar \left\{ \left[-\frac{1}{T} \theta(t'-t) t'(t+T) \hat{L}_{ij} \right. \right. \\ &\quad \left. \left. - \theta(t'-t) \frac{\sinh[t'\sqrt{-\nabla^2}] \sinh[(t+T)\sqrt{-\nabla^2}]}{\sqrt{-\nabla^2} \sinh[T\sqrt{-\nabla^2}]} \hat{T}_{ij} \right] \right. \\ &\quad \left. + (t \leftrightarrow t') \right\} \delta(\mathbf{x} - \mathbf{x}') \end{aligned} \quad (2.29)$$

is the usual temporal gauge finite-time propagator. The momentum space unsmeared field insertion $\hat{S}_i^a(\mathbf{p}, t)$ and propagator $\Delta_{ij}(\mathbf{p}; t, t')$ are represented as wavy line with small circle and wavy line respectively, as shown in fig. 2a and 2b.

The zeroth-order results (2.17) and (2.24) provide the basis for the diagrammatic expansions to be discussed in the next section.

$$= \tilde{S}_i^a(\vec{p}, t) \equiv \left[\frac{t+T}{T} \hat{L}_{ij} + \frac{\sinh[(t+T)p]}{\sinh[Tp]} \hat{T}_{ij} \right] A_j^a(\vec{p})$$

a

$$= \delta^{ab} \hbar \left\{ \left[-\frac{1}{T} \theta(t' - t)(t+T)t' \hat{L}_{ij} - \theta(t' - t) \frac{\sinh[(t+T)p] \sinh[t'p]}{p \sinh[Tp]} \hat{T}_{ij} \right] + (t \longleftrightarrow t') \right\}$$

b

$$= -\frac{ig}{\hbar} f^{abc} [(r - q)_i \delta_{jk} + (q - p)_k \delta_{ij} + (p - r)_j \delta_{ki}]$$

c

$$= -\frac{g^2}{\hbar} [f^{abn} f^{cdn} (\delta_{ik} \delta_{jl} - \delta_{il} \delta_{jk}) + f^{cbn} f^{adn} (\delta_{ik} \delta_{jl} - \delta_{ij} \delta_{lk}) + f^{dbn} f^{can} (\delta_{lk} \delta_{ij} - \delta_{jk} \delta_{li})]$$

c

Fig. 2. Feynman rules for $\tilde{Z}[A; T]$ (unsmearing case). (a) Unsmearing field insertion. (b) Unsmearing propagator. (c) Unsmearing vertices.

3. Diagrammatic expansions of the ground state

We now consider the perturbation series generated by the interaction factors in eqs. (2.17) for Z_ϕ and (2.24) for Z . Define

$$\tilde{Z}_\phi[A; T] \equiv Z_\phi^{(I)} \left[\frac{\delta}{\delta J} \right] Z_\phi^{(0)J}[A; T] \Big|_{J=0}, \tag{3.1a}$$

$$\tilde{Z}[A; T] \equiv Z^{(I)} \left[\frac{\delta}{\delta J} \right] Z^{(0)J}[A; T] \Big|_{J=0}, \tag{3.1b}$$

such that

$$Z_\phi[A; T] = \Gamma_\phi^{(0)}[A; T] \tilde{Z}_\phi[A; T], \quad Z[A, 0; T] = \Gamma^{(0)}[A; T] \tilde{Z}[A; T]. \quad (3.2)$$

With standard Feynman-diagrammatic arguments, it is easy to see that the quantity $\tilde{Z}_\phi - 1[\tilde{Z} - 1]$ in eqs. (3.1) are given by the sum of all possible connected and disconnected diagrams that can be constructed from the (t, \mathbf{p}) space finite-time Feynman rules of fig. 1 [fig. 2].

In these diagrams, the “legs” are the field insertions $\tilde{P}_i^a [\tilde{S}_i^a]$, and the finite-time propagators $\Delta_{ij}^\phi [\Delta_{ij}]$ can only appear as internal lines. Spatial momenta are conserved at all vertices, all momenta are integrated, intermediate times at the vertices are integrated from $-T$ to 0, and combinatoric factors are to be included in the usual manner.

If we denote the sum of all $O(g^r)$ diagrams that contribute to $\tilde{Z}_\phi [Z]$ by $D_r [\bar{D}_r]$, the diagrammatic expansions are represented by the equations,

$$\tilde{Z}_\phi[A; T] = \sum_{r=0}^{\infty} D_r, \quad \tilde{Z}[A; T] = \sum_{r=0}^{\infty} \bar{D}_r, \quad (3.3)$$

where $D_0 = \bar{D}_0 = 1$. In order to distinguish the diagrams that contribute to the wave functional from those that contribute to the energy, it is useful to consider the following two subclasses of $D_r [\bar{D}_r]$. For $r \geq 1$, let $D_r^P [\bar{D}_r^S]$ be the partial sum of $D_r [\bar{D}_r]$ that consists of all $O(g^r)$ diagrams in which there is at least one field insertion $\tilde{P}_i^a [\tilde{S}_i^a]$ in every connected subdiagram (these will contribute to the wave functional); and let $D_r^0 [\bar{D}_r^0]$ be the partial sum of $D_r [\bar{D}_r]$ in which there is no field insertion in any subdiagram (these will contribute to the energy). In fig. 3, we show a few examples of diagrams in these subclasses. In terms of these subclasses, it is clear that

$$D_r = \sum_{n=0}^r D_n^P D_{r-n}^0, \quad \bar{D}_r = \sum_{n=0}^r \bar{D}_n^S \bar{D}_{r-n}^0, \quad (3.4)$$

where for $r = 0$ we have adopted the convention

$$D_0^P = \bar{D}_0^S = D_0^0 = \bar{D}_0^0 = 1. \quad (3.5)$$

Eqs. (3.3)–(3.4) enable us to separate the wave functional and energy contributions into distinct factors,

$$\tilde{Z}_\phi[A; T] = \sum_{r=0}^{\infty} D_r = \left(\sum_{n=0}^{\infty} D_n^P \right) \left(\sum_{m=0}^{\infty} D_m^0 \right), \quad (3.6a)$$

$$\tilde{Z}[A; T] = \sum_{r=0}^{\infty} \bar{D}_r = \left(\sum_{n=0}^{\infty} \bar{D}_n^S \right) \left(\sum_{m=0}^{\infty} \bar{D}_m^0 \right). \quad (3.6b)$$

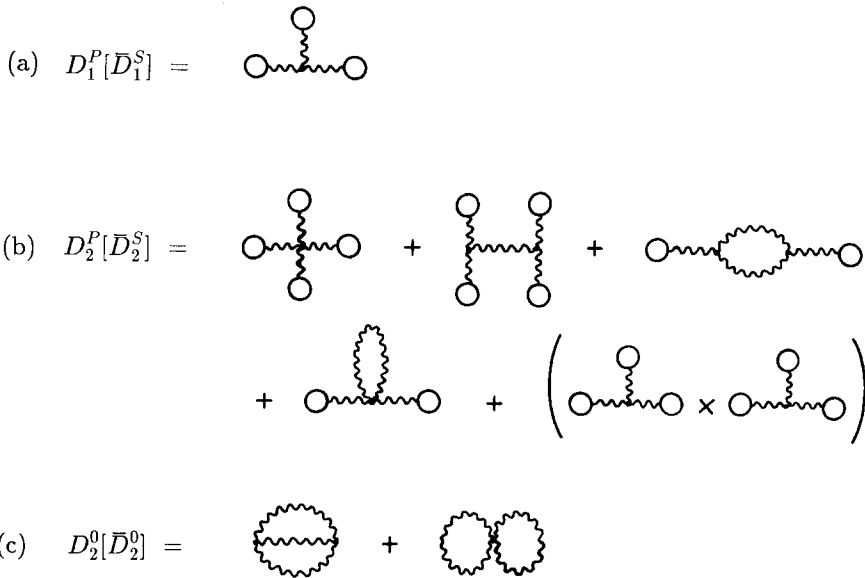


Fig. 3. Examples of the subclasses $D_r^P[\bar{D}_r^S]$ and $D_r^0[\bar{D}_r^0]$. The diagrams are to be computed by the Feynman rules of fig. 1 [fig. 2].

In particular, by setting the gauge field A to zero, we are left with only the diagrams that will contribute to the energy,

$$\tilde{Z}_\phi[0; T] = \sum_{r=0}^\infty D_r^0, \quad \tilde{Z}[0; T] = \sum_{r=0}^\infty \bar{D}_r^0. \tag{3.7}$$

Consequently, by eqs. (2.9)–(2.11) and (3.2), $W[A]$ is expressed in terms of the diagrammatic expansion of the functional $Z_\phi[Z]$ as

$$W[A] = W^{(0)}[A] + \hbar \lim_{T \rightarrow \infty} \ln \left(\sum_{r=0}^\infty D_r^P \right) \tag{3.8a}$$

$$= W^{(0)}[A] + \hbar \lim_{T \rightarrow \infty} \ln \left(\sum_{r=0}^\infty \bar{D}_r^S \right), \tag{3.8b}$$

where $W^{(0)}[A]$ is the zeroth-order result defined below. Then, by a standard argument in perturbation theory [12],

$$W[A] = W^{(0)}[A] + \hbar \lim_{T \rightarrow \infty} \sum_{r=1}^\infty D_{r,C}^P \tag{3.9a}$$

$$= W^{(0)}[A] + \hbar \lim_{T \rightarrow \infty} \sum_{r=1}^\infty \bar{D}_{r,C}^S, \tag{3.9b}$$

where $D_{r,C}^P [\bar{D}_{r,C}^S]$ is the sum of all *connected* diagrams among the diagrams of $D_r^P [\bar{D}_r^S]$. Note that the diagrams in $D_r^P [\bar{D}_r^S]$ which are products of connected parts, such as the last term of $D_2^P [\bar{D}_2^S]$ in fig. 3b, are excluded from $D_{r,C}^P [\bar{D}_{r,C}^S]$.

The corresponding expressions for the ground state energy are

$$E_0 = E_0^{(0)} - \hbar \lim_{T \rightarrow \infty} \frac{1}{T} \sum_{r=1}^{\infty} D_{r,C}^0 \tag{3.10a}$$

$$= E_0^{(0)} - \hbar \lim_{T \rightarrow \infty} \frac{1}{T} \sum_{r=1}^{\infty} \bar{D}_{r,C}^0, \tag{3.10b}$$

where $D_{r,C}^0 [\bar{D}_{r,C}^0]$ is the sum of all *connected* diagrams among $D_r^0 [\bar{D}_r^0]$, and $E_0^{(0)}$ is the zeroth-order result. Finally, the usual zeroth-order results may be computed from the expression for $\Gamma_{\Phi}^{(0)} [\Gamma^{(0)}]$ given in eqs. (2.18) [(2.25)],

$$W^{(0)}[A] = \hbar \lim_{T \rightarrow \infty} \left[\ln \frac{\Gamma_{\Phi}^{(0)}[A; T]}{\Gamma_{\Phi}^{(0)}[0; T]} \right] = \hbar \lim_{T \rightarrow \infty} \left[\ln \frac{\Gamma^{(0)}[A; T]}{\Gamma^{(0)}[0; T]} \right] \tag{3.11a}$$

$$= -\frac{1}{2} \int d\mathbf{x} A_i^{(T)a}(\mathbf{x}) \sqrt{-\nabla^2} A_i^{(T)a}(\mathbf{x}), \tag{3.11b}$$

$$E_0^{(0)} = -\hbar \lim_{T \rightarrow \infty} \frac{1}{T} \ln(\Gamma_{\Phi}^{(0)}[0; T]) = -\hbar \lim_{T \rightarrow \infty} \frac{1}{T} \ln(\Gamma^{(0)}[0; T]) \tag{3.12a}$$

$$= \hbar V(N^2 - 1) \int (d\mathbf{p}) p. \tag{3.12b}$$

All contributions to $W[A]$ and E_0 are now given in terms of diagrams, except for the first order, by eqs. (3.9)–(3.10). To uniformize the diagrammatic picture, we also introduce *ad hoc* diagrams for $W^{(0)}[A]$ and $E_0^{(0)}$, as given in fig. 4.

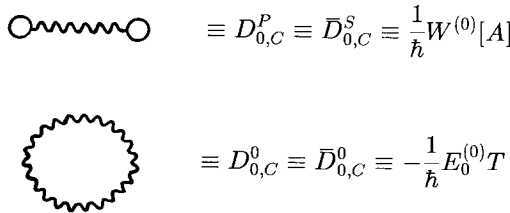


Fig. 4. *Ad hoc* representations for $W^{(0)}[A]$ and $E_0^{(0)}$.

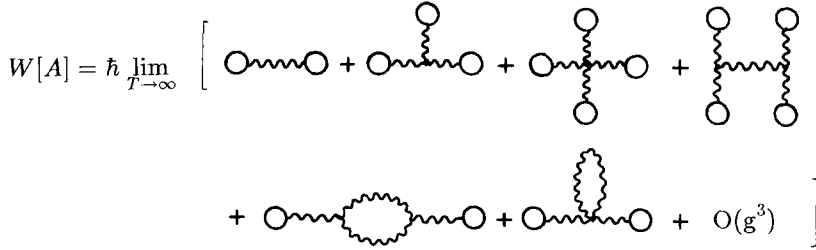


Fig. 5. Connected diagrammatic expansion for $W[A]$.

With this convention, we may write the following expressions for the $O(g')$ terms in $W[A]$ and E_0 ,

$$W^{(r)}[A] = \hbar \lim_{T \rightarrow \infty} D_{r,C}^P = \hbar \lim_{T \rightarrow \infty} \bar{D}_{r,C}^S, \tag{3.13a}$$

$$E_0^{(r)} = -\hbar \lim_{T \rightarrow \infty} \frac{1}{T} D_{r,C}^0 = -\hbar \lim_{T \rightarrow \infty} \frac{1}{T} \bar{D}_{r,C}^0. \tag{3.13b}$$

We shall refer to $D_{r,C}^P$ or $\bar{D}_{r,C}^S$ as wave functional diagrams and $D_{r,C}^0$ or $\bar{D}_{r,C}^0$ as energy diagrams. Their explicit diagrammatic representations are illustrated by figs. 5 and 6.

Either set of the Feynman rules of fig. 1 and 2 may be used for the computation of these diagrams. Aside from the additional connectedness requirement, they are constructed by the prescription given in the beginning of this section. As in usual finite-time Feynman diagrams [9], one must perform all computations at finite time, leaving the $T \rightarrow \infty$ limit until last. In the next section, we will apply these rules to determine the first-order wave functional.

The diagrammatic perturbative expansions above may also be organized as semi-classical expansions. Consider the semi-classical expansions

$$W[A] = \sum_{r=0}^{\infty} \hbar^r W_r[A], \tag{3.14a}$$

$$E_0 = \sum_{r=0}^{\infty} \hbar^r E_{0,r}, \tag{3.14b}$$

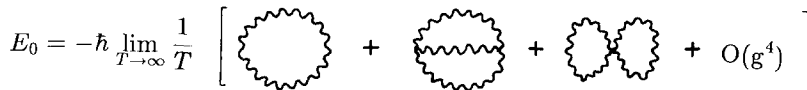


Fig. 6. Connected diagrammatic expansion for E_0 .

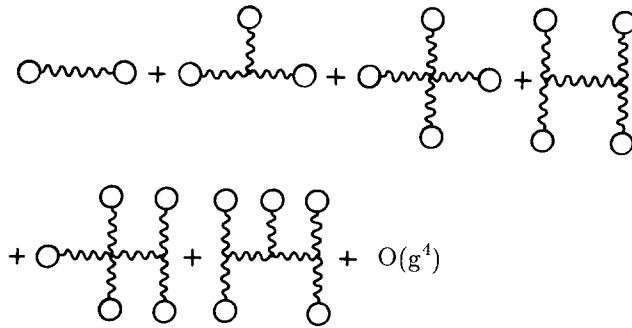


Fig. 7. W_0/\hbar is the sum of all tree diagrams at large T .

in which $W_r[A]$ and $E_{0,r}$ are respectively $O(\hbar^r)$ contributions to $W[A]$ and E_0 . Making use of the fact that propagators are $O(\hbar)$, field insertions are $O(\hbar^0)$, and vertices are $O(\hbar^{-1})$, it follows from standard diagrammatic arguments [13] that diagrams with r loops contribute to $W[A]$ and E_0 at order \hbar^r . More precisely, $W_r[A]$ and E_r are respectively the sum of all wave functional and energy diagrams with r internal loops.

For the energy diagrams, the order in g and \hbar are directly related by

$$E_0^{(2r)} = E_{0,r+1}, \quad r \geq 0. \tag{3.15}$$

Also, it is easy to deduce from the Feynman rules that there is no energy diagram that contributes to any odd order in g , and that $E_{0,0} = 0$.

In the case of the wave functional, however, $W_r[A]$ in general contains an infinite number of diagrams. This is because there are always r -loop wave functional diagrams if the order in g is greater than or equal to r . In particular, the lowest approximation in \hbar , $W_0[A]$, is the sum of all tree diagrams, which is illustrated in fig. 7 by its partial sum through $O(g^3)$.

Substituting the expansions (3.14) into the Schrödinger equation (2.6) and equating terms of order \hbar^0 , we find that the sum of all tree diagrams satisfies

$$\frac{1}{2} \int d\mathbf{x} \left[\frac{\delta W_0}{\delta A_i^a(\mathbf{x})} \frac{\delta W_0}{\delta A_i^a(\mathbf{x})} - B_i^a(\mathbf{x}) B_i^a(\mathbf{x}) \right] = 0, \tag{3.16}$$

which is the zero-energy Hamilton-Jacobi equation of classical mechanics. To obtain this result we used the fact that $E_{0,0} = 0$.

In this connection, we note that similar expansions may be useful in studying the conjecture of Claudson and Halpern [14] that supersymmetric ground state wave functions are generally much simpler than those of non-supersymmetric systems. Indeed, Claudson and Halpern have found broad classes of examples in which the semi-classical series terminates, and exact ground states are obtained.

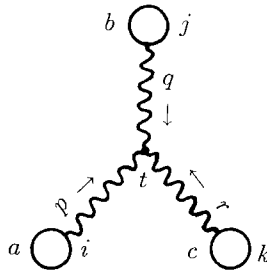


Fig. 8. $O(g)$ wave functional diagram.

4. The first-order ground state wave functional

As an application of the diagrammatic rules, we compute $W[A]$ and E_0 through first order in g . Since it is impossible to construct an $O(g)$ energy diagram, we conclude that $E_0^{(1)} = 0$.

The only diagram that contributes to $W^{(1)}[A]$ is the tree diagram of fig. 8. From the Feynman rules of fig. 1, an expression for $W^{(1)}[A]$ is written down immediately,

$$\begin{aligned}
 W^{(1)}[A] = \hbar \lim_{T \rightarrow \infty} & \left\{ \frac{1}{3!} \int_{-T}^0 dt \int (d\mathbf{p})(d\mathbf{q})(d\mathbf{r})(2\pi)^3 \delta(\mathbf{p} + \mathbf{q} + \mathbf{r}) \right. \\
 & \times \frac{1}{\hbar} \left[-igf^{abc} \left(1 + \frac{\delta(t)}{\epsilon^2} \right) \right] \left[(r - q)_i \delta_{jk} + (q - p)_k \delta_{ij} + (p - r)_j \delta_{ki} \right] \\
 & \left. \times \tilde{P}_i^a(\mathbf{p}, t) \tilde{P}_j^b(\mathbf{q}, t) \tilde{P}_k^c(\mathbf{r}, t) \right\}. \tag{4.1}
 \end{aligned}$$

In the above expression, $1/3!$ is the combinatoric factor associated with three identical field insertions in the diagram. Inside the spatial momentum integral, the δ -function enforces momentum conservation at the vertex. As stated above, all time integrations must be done before taking the infinite T limit. In this diagram, these integrations are straightforward: For example, from the product of two longitudinal insertions with one transverse insertion, we encounter

$$\lim_{T \rightarrow \infty} \int_{-T}^0 dt \left(1 + \frac{\delta(t)}{\epsilon^2} \right) \frac{-p \sinh(tp) + \epsilon^2 \cosh(tp)}{p \sinh(Tp) + \epsilon^2 \cosh(Tp)} = \frac{1}{p}. \tag{4.2}$$

After performing all time integrations and taking the infinite T limit, the result is seen to be independent of ϵ^2 . Terms are then grouped by permutation of integration

variables and indices. Finally, we arrive at the relatively compact form

$$\begin{aligned}
 W^{(1)}[A] = & -\frac{1}{6}igf^{abc} \int (d\mathbf{p})(d\mathbf{q})(d\mathbf{r})(2\pi)^3 \delta(\mathbf{p} + \mathbf{q} + \mathbf{r}) \\
 & \times \left[(r - q)_i \delta_{jk} + (q - p)_k \delta_{ij} + (p - r)_j \delta_{ki} \right] \\
 & \times \left\{ \frac{3}{p} \left[A_i^{(T)a}(\mathbf{p}) A_j^{(L)b}(\mathbf{q}) A_k^{(L)c}(\mathbf{r}) \right] \right. \\
 & \quad + \frac{3}{p + q} \left[A_i^{(T)a}(\mathbf{p}) A_j^{(T)b}(\mathbf{q}) A_k^{(L)c}(\mathbf{r}) \right] \\
 & \quad \left. + \frac{1}{p + q + r} \left[A_i^{(T)a}(\mathbf{p}) A_j^{(T)b}(\mathbf{q}) A_k^{(T)c}(\mathbf{r}) \right] \right\}. \tag{4.3}
 \end{aligned}$$

The inverse momentum factors arise from time integrations, such as that in eq. (4.2), and they are certainly akin to the energy denominators of hamiltonian perturbation theory. A similar computation using the unsmeared Feynman rules of fig. 2 yields exactly the same result.

It can easily be verified that $W^{(1)}[A]$ is real, and that $\exp[W^{(0)} + W^{(1)}]$ satisfies both the Schrödinger equation (2.6) and the Gauss' law condition (2.7) through first order in g . The computation with the Schrödinger equation reconfirms that $E_0^{(1)} = 0$.

With considerable algebra, we checked that our result (4.3) and that of Hatfield's [4] are in agreement. We emphasize however that our method is systematic, involving no guess work, and is in principle applicable to all orders.

We finally comment on the notion of "gauge-invariant completion". At any order in our systematic perturbative expansion, the result satisfies Gauss' law only perturbatively. Therefore, finding a gauge-invariant form which agrees with perturbation theory to that order is a way of improving perturbation theory. As an example, we have been successful in finding a gauge-invariant completion of our first-order result above:

$$\begin{aligned}
 W_{GI}[A] = & -\frac{1}{2} \int d\mathbf{x} d\mathbf{y} (\mathbf{D} \times \mathbf{B})_i^a(\mathbf{x}) \left[\left(\frac{1}{-D^2} \right)^{3/2} \right]_{xy}^{ab} (\mathbf{D} \times \mathbf{B})_i^b(\mathbf{y}) \\
 & - g \int d\mathbf{x} d\mathbf{y} d\mathbf{z} \hat{O}_{xyz}^{abc} \left[D_j^{ad} (\mathbf{D} \times \mathbf{B})_i^d(\mathbf{x}) \right] (\mathbf{D} \times \mathbf{B})_i^b(\mathbf{y}) (\mathbf{D} \times \mathbf{B})_j^c(\mathbf{z}) \\
 = & W^{(0)}[A] + W^{(1)}[A] + O(g^2), \tag{4.4}
 \end{aligned}$$

where

$$(D^2)^{ab} \equiv D_i^{ac} D_i^{cb}, \quad (\mathbf{D} \times \mathbf{B})_i^a \equiv \epsilon_{ijk} D_j^{ab} B_k^b. \tag{4.5}$$

The operator \hat{O}_{xyz}^{abc} is defined as follows.

$$\hat{O}_{xyz}^{abc} = \hat{M}_{xyz}^{abc} - \hat{N}_{xyz}^{abc} - \hat{R}_{xyz}^{abc}, \quad (4.6)$$

where \hat{M} , \hat{N} , and \hat{R} are defined by the equations,

$$\begin{aligned} \int d\mathbf{x}' d\mathbf{y}' d\mathbf{z}' \left[(\tilde{D})_{xx'; yy'; zz'}^{aa'; bb'; cc'} + (\tilde{D})_{yy'; zz'; xx'}^{bb'; cc'; aa'} + (\tilde{D})_{zz'; xx'; yy'}^{cc'; aa'; bb'} \right] \hat{M}_{x'y'z'}^{a'b'c'} &= f^{abc} \delta_{xz} \delta_{yz}, \\ \int d\mathbf{x}' d\mathbf{y}' d\mathbf{z}' \left[(\tilde{D})_{xx'; yy'; zz'}^{aa'; bb'; cc'} + (\tilde{D})_{yy'; zz'; xx'}^{bb'; cc'; aa'} \right] \hat{N}_{x'y'z'}^{a'b'c'} &= f^{abc} \delta_{xz} \delta_{yz}, \\ \int d\mathbf{x}' d\mathbf{y}' d\mathbf{z}' \left[(\tilde{D})_{zz'; xx'; yy'}^{cc'; aa'; bb'} \right] \hat{R}_{x'y'z'}^{a'b'c'} &= f^{abc} \delta_{xz} \delta_{yz}, \end{aligned} \quad (4.7)$$

and

$$(\tilde{D})_{xx'; yy'; zz'}^{aa'; bb'; cc'} \equiv [(-D^2)^{3/2}]_{xx'}^{aa'} [-D^2]_{yy'}^{bb'} [-D^2]_{zz'}^{cc'}, \quad \delta_{xz} \equiv \delta(\mathbf{x} - \mathbf{z}). \quad (4.8)$$

Note that $W^{(0)} + W^{(1)}$ is of order \hbar^0 , since both terms come from tree graphs, while the gauge-invariant completion W_{GI} has added only terms of order \hbar^0 , since the covariant derivative is independent of \hbar . It follows that W_{GI} is a partial summation of pieces of the tree diagrams to all orders in g . In general, since gauge transformations are classical (no factors of \hbar), a gauge-invariant completion (via covariant derivatives) of a sum of low order graphs of a given loop number is a partial summation of pieces of graphs to all orders in g at that loop number.

Unfortunately, with further guess work, we have found another gauge-invariant completion, which for brevity we will not give here, so the completion is not unique at this order. In other words, the completion eq. (4.4) does not satisfy the Hamilton-Jacobi equation (3.16).

It would be interesting to study the uniqueness of the gauge-invariant completion after second-order perturbation theory. In particular, there are both tree diagrams and one-loop diagrams at second order, so one gets another chance to determine the sum of tree diagrams at this order, and a first chance at summation of one-loop diagrams. We finally mention that, as a method, gauge-invariant completion of perturbation theory seems ideally suited to study the Claudson-Halpern conjecture [14] in supersymmetric QCD.

I wish to thank Prof. M.B. Halpern for suggesting this problem, and for many helpful discussions and advice. I also thank Zvi Bern for helpful discussions. This work was supported by the Director, Office of Energy Research, Office of High

Energy and Nuclear Physics, Division of High Energy Physics of the US Department of Energy under contract DE-AC03-76SF00098 and the National Science Foundation under Research Grant No. PHY-85-15857.

References

- [1] H. Loos, *Phys. Rev.* 188 (1969) 2342
- [2] J.P. Greensite, *Nucl. Phys.* B158 (1979) 469
- [3] S. Nojiri, *Z. Phys.* C22 (1984) 245
- [4] B.F. Hatfield, *Phys. Lett.* 147B (1984) 435
- [5] J.P. Greensite and M.B. Halpern, *Nucl. Phys.* B259 (1985) 90;
J.P. Greensite and M.B. Halpern, *Nucl. Phys.* B271 (1986) 379
- [6] G.C. Rossi and M. Testa, *Nucl. Phys.* B163 (1980) 109
- [7] G.C. Rossi and M. Testa, *Nucl. Phys.* B176 (1980) 477
- [8] Z. Bern and H.S. Chan, *Nucl. Phys.* B266 (1986) 509
- [9] H.S. Chan, preprint LBL-20625, *Phys. Rev. D*, to be published
- [10] R.P. Feynman, *Nucl. Phys.* B188 (1981) 479
- [11] M. Claudson and M.B. Halpern, *Phys. Lett.* 151B (1985) 281
- [12] P. Ramond, *Field theory, a modern primer* (Benjamin/Cummings, Massachusetts, 1981)
- [13] C. Itzykson and J. Zuber, *Quantum field theory* (McGraw-Hill, 1980)
- [14] M. Claudson and M.B. Halpern, *Nucl. Phys.* B250 (1985) 689